

Central Lancashire Online Knowledge (CLoK)

Title	Influence of transient nonlinear behaviour of lubricant stiffness and
	damping upon transmission gear rattle
Type	Article
URL	https://knowledge.lancashire.ac.uk/id/eprint/57256/
DOI	https://doi.org/10.1115/1.4070170
Date	2026
Citation	Rahnejat, Homer, Johns-Rahnejat, Patricia and Dolatabadi, N. (2026) Influence of transient nonlinear behaviour of lubricant stiffness and damping upon transmission gear rattle. Journal of Tribology, 148 (3). 034603. ISSN 0742-4787
Creators	Rahnejat, Homer, Johns-Rahnejat, Patricia and Dolatabadi, N.

It is advisable to refer to the publisher's version if you intend to cite from the work. https://doi.org/10.1115/1.4070170

For information about Research at UCLan please go to http://www.uclan.ac.uk/research/

All outputs in CLoK are protected by Intellectual Property Rights law, including Copyright law. Copyright, IPR and Moral Rights for the works on this site are retained by the individual authors and/or other copyright owners. Terms and conditions for use of this material are defined in the http://clok.uclan.ac.uk/policies/

Influence of transient nonlinear behaviour of lubricant stiffness and damping upon transmission gear rattle

H. Rahnejat^{1,2}, P.M. Johns-Rahnejat¹ and N. Dolatabadi^{2*}

¹ School of Engineering, University of Lancashire, Preston, UK
² Wolfson School of Mechanical, Electrical and Manufacturing Engineering, Loughborough University, Loughborough, UK
*Corresponding Author: N.Dolatabadi@lboro.ac.uk

Abstract

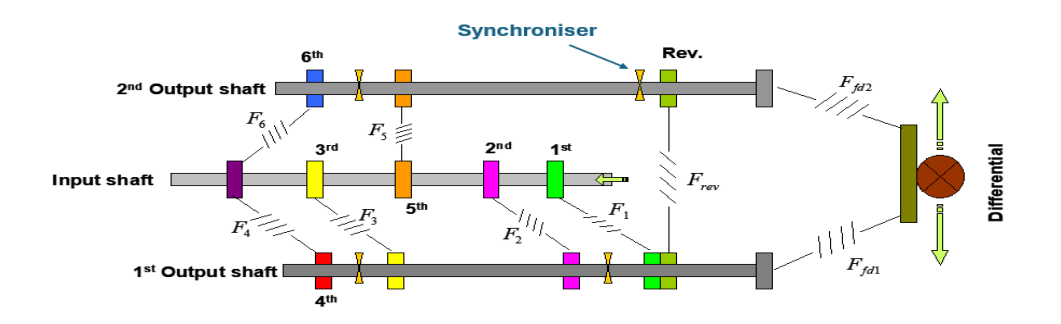
Transmission rattle occurs in light-to-medium loaded interactions of loose gear pairs when subjected to vibration. The paper provides solutions for iso-viscous and piezo-viscous hydrodynamic lubricant behaviour that are an underlying cause of gear rattle. The non-linear stiffness and damping characteristics are obtained and their variation under transient conditions in combined rolling, and normal approach and separating contacts are discussed. Relationships for lubricant reaction under both lightly loaded iso-viscous and medium loaded piezo-viscous conditions are determined, the latter for the first time for the case of counterformal line contact geometries. The underlying reason for idle rattle, a significant concern in vehicular transmissions, is explained in a fundamental manner through unstable spectral content of lubricant film surface ripple oscillations. As transmitted load increases during vehicle launch, piezo-viscous behaviour suppresses these instabilities, inducing creep rattle during the transition from idle to drive rattle. Thus, the fundamental role of lubricant behaviour in influencing transmission rattle has been demonstrated, which has not hitherto been reported in the literature.

Keywords: Transmission gear rattle, idle rattle, creep rattle, non-linear stiffness; non-linear damping; intermittent impacts, Transient non-conforming lubricated line contacts

1- Introduction

In recent times there has been a growing trend towards high output power- to weight ratio in the development of propulsion systems such as vehicular engines and transmissions. One approach has been system and component downsizing. For gearing transmissions, the reduced separation of input and output shafts has resulted in repetitive impact of unselected (unengaged loose gears) at light impact loads. This results in propagation of noise from the impact zones, termed rattle in the automotive industry. The case of idle gear rattle occurs when no meshing gear pair exist (vehicle idling) (figure 1). The impact zones are shown in the figure. In idle rattle the impact forces are insufficient to promote lubricant piezo-viscous behaviour (i.e. the lubricant response is iso-viscous hydrodynamics). Idle gear

rattle is quite audible due to low engine noise under vehicle stationary idling condition [2-5]. It has been a major source of noise, vibration and harshness (NVH) concern in the industry [6].



F: Gear Ratios

All gear pairs unengaged

Figure 1: 6-speed vehicular transmission under idle rattle condition

As the transmission is engaged in first or second gear, engine power is increased (at the onset of vehicle launch). The unengaged gear pairs are then subjected to higher impact forces, promoting piezo-viscous hydrodynamics. The impact force is insufficient to induce any localised deformation of surfaces (see later), which would be necessary for inception of elastohydrodynamic (EHD) conditions. The engaged gear pairs transmit much higher contact forces, resulting in EHD. Gear rattle still occurs with engaged gear pairs (because of existing backlash) but is not usually heard owing to the high engine sound accompanying increased output power. Rattle from engaged gear pairs at high load is termed drive rattle [7]. Various forms of transmission rattle were described in some detail with some descriptive emphasis on the role of lubricant by Menday [8]. However, the fundamental behaviour of the lubricant underlying rattle characteristics has not, hitherto, been evaluated.

The dynamics of systems where the load is supported or transmitted through lubricated contacts is complicated because, at each step of simulation, combined solution of the inertial dynamics equation of motion and mechanics of lubricated contacts is required. Such tribodynamics analyses often require the numerical solution of Reynolds equation, which can be inordinately time-consuming. Rattle is just one such problem. Other similar problems include non-conforming contacts, where the contact footprint can be characterised by a long and narrow rectangular strip. For example; cam-tappet contact [9-12]; a pair of meshing spur gear teeth [13-17]; piston ring and cylinder liner (when the contact is viewed as unwrapped) [18-20]; or misaligned concentrated contact of cylindrical joints [21, 22]. In dynamic analyses, the contacts are often represented by spring-damper restoring reactions in the equations of

motion. However, in lubricated contacts the stiffness and damping characteristics are non-linear and often cannot easily be represented by separate restoring elements.

In all cases, the contacting surfaces are subjected to relative rolling-sliding motion with mutual convergence and separation of surfaces, such as in the meshing of gear teeth, or in the traverse of rolling elements from the loaded into the unloaded regions of a bearing [23-26]. The normal approach and separation of contacting surfaces gives rise to squeeze film action, which is often omitted in lubricated contact analysis but is essential under transient conditions (i.e. for all dynamic studies) [27-29]. The squeeze film motion is a transient phenomenon which promotes lubricant film damping contribution and increases the contact load carrying capacity [30]. Therefore, the solution of Reynolds equation for dynamic analyses (i.e. tribodynamics) should include the effect of squeeze film motion.

In many cases, the development of non-linear stiffness and damping elements from numerical/analytical results of lubricated contacts provides the opportunity for time-efficient tribodynamic analysis under transient conditions, such as in transmission gear rattle. The procedure was first highlighted in [31] for ball-race contacts in bearings as the ball complement undergo their orbital motion subjected to transient changes in the prevailing regimes of lubrication. To provide a numerical solution for a cage cycle of several lubricated ball-to-races contacts would be computationally prohibitive. There have been a number of studies to predict or develop stiffness and damping characteristics of lubricated contacts, mostly for highly loaded cases under elastohydrodynamic regime of lubrication (EHL: piezo-viscous elastic) [16, 32-36]. Lubricant film damping, arising from squeeze film motion, has been found to be rather insignificant under EHL [37, 38]. Thicker films under hydrodynamic regimes of lubrication provide more damping through the dissipation of energy, as already shown in phase plane representations for ball bearing dynamics [31].

There has been a dearth of analysis of stiffness and damping characteristics of non-conforming line contacts under hydrodynamic regime of lubrication. Yet, many contacts at light to medium loads such as gearing transmissions are subject to this condition, leading to rattle and clatter phenomena, which, as already mentioned, is a major industrial concern [1-6]. In general, light to medium loaded lubricated line contacts fall within iso-viscous or piezo-viscous rigid regimes of lubrication. As already noted, these conditions occur in a host of lubricated conjunctions. Therefore, the determination of stiffness and damping characteristics of such contacts in combined rolling-sliding and squeeze film motions would advance tribodynamic analyses.

This paper provides analytical solutions for light-to-medium loaded non-conforming transient hydrodynamic line contacts and develops non-linear stiffness and damping elements, an approach not hitherto reported in the open literature. Subsequent detailed dynamic analysis of gearing transmission

under low impacting loads, pertaining to gear rattle conditions, is provided. Transient hydrodynamic lubricant behaviour is shown to be the underlying cause of differing gear rattle classifications.

2- Tribodynamics of loose gear pair lightly-loaded impact

As already noted, the impact of loose (unselected/unengaged) gear pairs leads to the phenomenon of gear rattle. The equation of motion can be stated as:

$$\ddot{z} = \frac{1}{m} \{ W(t) - F(t) \} - g \tag{1}$$

where, W(t) is the lubricant hydrodynamic reaction, F(t) is the impact force, m is the equivalent mass of the impacting teeth pair, g is the gravitational acceleration and \ddot{z} is the acceleration of the loose gear surface. Note that the impact of a pair of loose gear teeth is considered as two instantaneous impacting cylinders. In contact mechanical terms this is the same as a rigid cylinder of equivalent radius, R (figure 2) impacting a semi-infinite elastic half-space of effective Young's modulus of elasticity, E^* , where:

$$\frac{1}{R} = \frac{1}{r_1} + \frac{1}{r_2} \tag{2}$$

For two surfaces of the same material, the plane strain equivalent modulus is:

$$E^* = \frac{E}{1 - \theta^2} \tag{3}$$

where, ϑ is the Poisson's ratio.

The impact force for loose gear pairs is low in magnitude, not causing any localised deformation of teeth surfaces. These conditions pertain to lightly loaded hydrodynamics, mostly under iso-viscous condition as the generated pressures are fairly insufficient to promote piezo-viscous action of the lubricant. Typical data concerning the impact geometry, R, material properties, E, θ , η , and operating conditions, u, w, F are used to determine the fluid film regime of lubrication (see section 3). It can be seen that the maximum generated pressure at highest squeeze film velocity does not exceed 200 MPa (see figure 5). The solidification pressure of most transmission fluids is around 300 MPa [39], where the lubricant acts as an amorphous solid (a pre-requisite of elastohydrodynamic regime of lubrication). Furthermore, using the classical Hertzian contact mechanics [40] for idealised counterformal line contact, the localised contact deflection becomes:

$$\delta = \frac{4Rp^2}{E^{*2}} \tag{4}$$

For $E^* = 226$ GPa, R = 0.0127 m, p = 200 MPa: $\delta = 0.04$ µm, which is negligible. Hence, the prevailing conditions are piezo-viscous hydrodynamics. Therefore, as already stated by many authors, gear rattle occurs under light-to-medium loaded hydrodynamics [1-6, 8]. Under hydrodynamic conditions and at light to medium load surface roughness effects are negligible. Therefore, smooth surfaces are assumed.

3- Analytical model for hydrodynamic line contacts

To obtain a solution for the equation of motion (1), one needs an expression for the lubricant reaction, W(t), which is a combination of lubricant restoring stiffness and damping actions. The reaction is required at any instant of time in the normal approach and separation of the impacting teeth and in their in-situ relative rolling and sliding motion. This is a transient phenomenon, for which a solution of Reynolds hydrodynamic equation is required. Generic numerical solutions of Reynolds equation have been reported ever since the pioneering contribution of Dowson [41]. However, no analytical solutions suitable for inclusion in time-efficient tribodynamics analysis under transient conditions have been reported for the case of non-conforming contacts (as in the contact of gear teeth pairs). For the case of conforming contact of journal bearings as in infinitely long bearing or infinitesimally short bearing analytical conditions for steady state rolling have been reported and are now well-known textbook contributions.

The general case of a non-conforming line contact may be viewed as a pair of idealised right circular cylinders in axial contact (figure 2). The contact footprint is a long rectangular strip when the cylinders have a large length-to-diameter ratio. If this ratio is very large, the pressure variation in the axial direction, y, may be considered as insignificant compared with the pressure gradient in the lateral rolling direction, x. This condition is referred to as idealised infinite line contact. A one-dimensional solution of Reynolds equation would suffice in this case. For the case of rolling and squeeze film motions with no side leakage of lubricant:

$$\frac{\partial}{\partial x} \left(\frac{h^3}{\eta} \frac{dp}{dx} \right) = 12 \left\{ (u_1 + u_2) \frac{\partial h}{\partial x} + (w_1 - w_2) \right\} \tag{5}$$

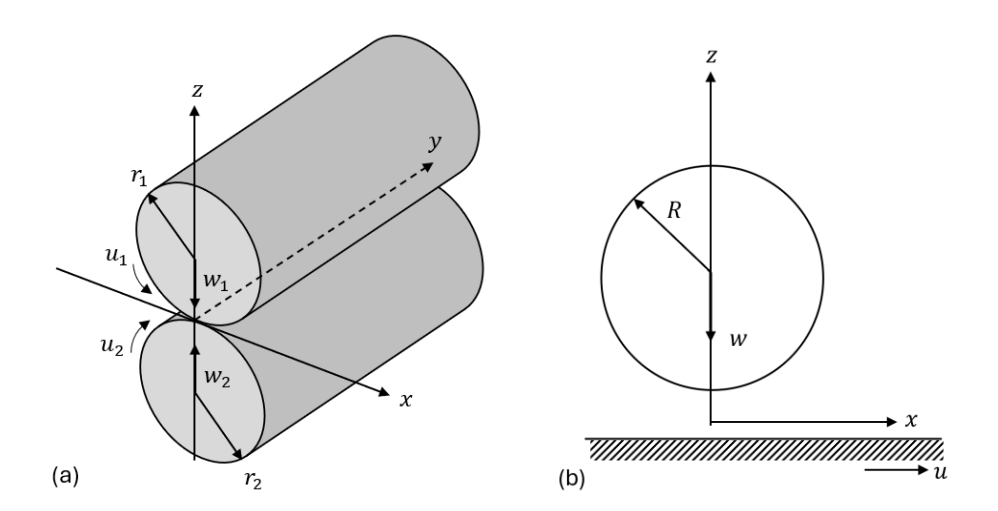


Figure 2: Schematic representation of (a) counterformal line contact and (b) idealised representation

3.1- Iso-viscous condition: Pressure distribution and load carrying capacity

For iso-viscous condition: $\eta = \eta_0$.

Let $u = \frac{1}{2}(u_1 + u_2)$, and $w = w_1 - w_2$, thus:

$$\frac{\partial}{\partial x} \left(h^3 \frac{dp}{dx} \right) = 6 \, \eta_0 \left\{ u \frac{\partial h}{\partial x} + 2w \right\} \tag{6}$$

Integrating twice with respect to x and using the following boundary conditions:

$$\frac{dp}{dx} = 0 \text{ at } x = -x_a \tag{7}$$

where:

$$p = p_0 \text{ and } h = h_a \tag{8}$$

The pressure gradient becomes:

$$\frac{dp}{dx} = \frac{6u\eta_0(h - h_a)}{h^3} + \frac{12w\eta_0(x + x_a)}{h^3} \tag{9}$$

The film shape for an equivalent ellipsoidal solid of revolution of radius R (for the contacting cylinders in Figure 2) against a flat surface is parabolic, thus:

$$h = h_0 \left(1 + \frac{x^2}{2Rh_0} \right) \tag{10}$$

Replacing for film thickness from equation (10) into equation (9) yields:

$$\frac{dp}{dx} = \frac{6\eta_0}{h_0^3 \left\{ 1 + \left(\frac{x^2}{2Rh_0}\right) \right\}^3} \left\{ \frac{u}{2R} \left(x^2 - x_a^2 \right) + 2w(x + x_a) \right\}$$
 (11)

The following non-dimensional terms are used to provide a generic dimensionless form of the idealised non-conforming line contact hydrodynamic Reynolds equation:

$$tan\bar{x} = \frac{x}{(2Rh_0)^{1/2}}, \ tan\bar{x}_a = \frac{x_a}{(2Rh_a)^{1/2}}, \ w^* = \frac{w}{u}, \ p^* = \frac{h_0^{3/2}p}{6\sqrt{2R}u\eta_0}, \ h_0^* = \frac{h_0}{R}$$
 (12)

Also:
$$dx = \sqrt{2Rh_0} \sec^2 \bar{x} d\bar{x}$$
 and $d\bar{x}_a = 0$ (13)

Substituting from (9) and (10) into (8) yields:

$$\frac{dp^*}{d\bar{x}} = \sin^2 \bar{x} \cos^2 \bar{x} - \tan^2 \overline{x_a} \cos^4 \bar{x} + \frac{4w^*}{\sqrt{2h_0^*}} (\sin \bar{x} \cos^2 \bar{x} + \tan \overline{x_a} \cos^4 \bar{x})$$
 (14)

Now integrating with respect to \bar{x} and using the following boundary condition for a fully flooded inlet:

$$p^* = 0$$
 at $\bar{x} = -\frac{\pi}{2}$ (corresponding to $p = 0$ at $x = -\infty$) (15)

yields:

$$p^* = \frac{1}{8}\bar{x} - \frac{1}{32}\sin 4\bar{x} - \tan^2 \overline{x_a} \left(\frac{3}{8}\bar{x} + \frac{1}{4}\sin 2\bar{x} + \frac{1}{32}\sin 4\bar{x}\right) + \frac{4w^*}{\sqrt{2h_0^*}} \left\{-\frac{3}{2} - \frac{1}{8}\cos 2\bar{x} - \frac{1}{32}\cos 4\bar{x} + \tan \overline{x_a} \left(\frac{3}{8} + \frac{1}{4}\sin 2\bar{x} + \frac{1}{32}\sin 4\bar{x}\right)\right\} + \frac{\pi}{16} \left(1 - 3\tan^2 \overline{x_a} + \frac{12w^*}{\sqrt{2h_0^*}}\tan \overline{x_a}\right)$$

$$(16)$$

Clearly, the pressure distribution in equation (16) is dependent on the position $\overline{x_a}$. This position may be determined by the boundary condition: $p^* = 0$ at $\overline{x} = \frac{\pi}{2}$ (full Sommerfeld condition). However, this condition leads to the erroneous zero load carrying capacity. Therefore, the following boundary condition for lubricant film rupture at the exit from the contact can be used, using the Swift [42] - Stieber [43] boundary conditions, where $-\overline{x_a}$ is replaced by $\overline{x_e}$ in equation (16):

$$p^* = \frac{dp^*}{d\bar{x}} = 0 \quad at \ \bar{x} = \overline{x_e} \tag{17}$$

Applying the above oil film rupture position to equation (16) yields a non-linear equation which enables the determination of $\overline{x_e}$ for any given value of squeeze-roll kinematic speed ratio, w^* , and the minimum dimensionless separation, h_0^* , using numerical successive substitution technique:

$$\frac{1}{8}\overline{x_e} - \frac{1}{32}\sin 4\overline{x_e} - \tan^2\overline{x_e}\left(\frac{3}{8}\overline{x_e} + \frac{1}{4}\sin 2\overline{x_e} + \frac{1}{32}\sin 4\overline{x_e}\right) + \frac{4w^*}{\sqrt{2h_0^*}}\left\{-\frac{3}{2} - \frac{1}{8}\cos 2\overline{x_e} - \frac{1}{32}\cos 4\overline{x_e} + \tan\overline{x_e}\left(\frac{3}{8}\overline{x_e} + \frac{1}{4}\sin 2\overline{x_e} + \frac{1}{32}\sin 4\overline{x_e}\right)\right\} + \frac{\pi}{16}\left(1 - 3\tan^2\overline{x_e} + \frac{12w^*}{\sqrt{2h_0^*}}\tan\overline{x_e}\right) = 0$$
(18)

With increasing w^* the position of maximum pressure $\bar{x} = -\overline{x_a} \to 0$ (position of pure squeeze, $w^* \to \infty$), whereas for the position of film rupture: $\overline{x_e} \to \frac{\pi}{2}$ (full Sommerfeld exit boundary). However, for

most hydrodynamic conjunctions: $w^* < -10^{-3}$, where negative values of w^* indicate normal approach of surfaces (figure 3).

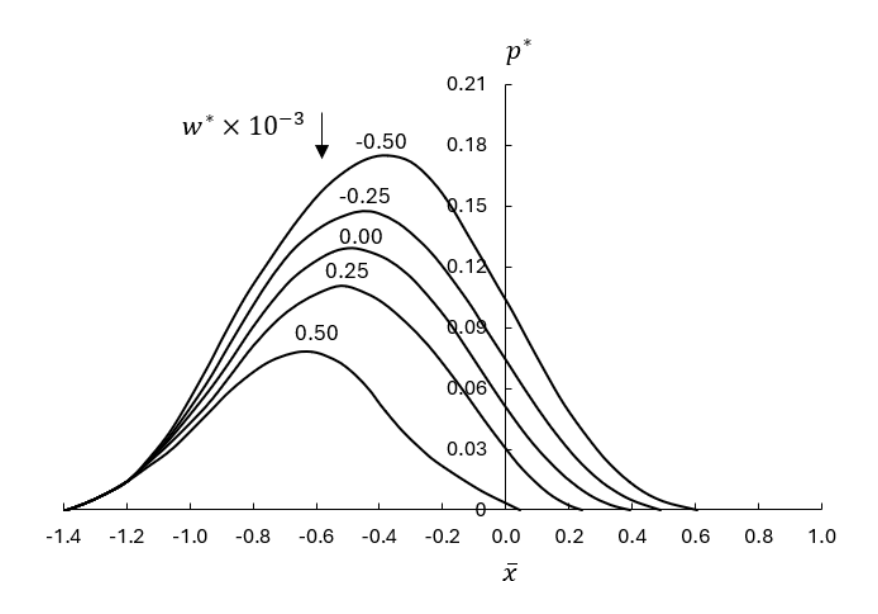


Figure 3: Dimensionless iso-viscous pressure distribution (combined Reynolds rolling condition and squeeze effect)

It can be seen that with normally approaching surfaces ($w^* < 0$), the load carrying capacity (area under the pressure distribution) is increased from the case of pure rolling ($w^* = 0$) for the same minimum separation, h_0^* . For the cases where $w^* > 0$, the surfaces are in a state of separation. This leads to reduced pressures and, therefore, decreased load carrying capacity.

The generated contact load per unit length can be obtained as:

$$\frac{W}{l} = \int_{x_l}^{x_e} p dx \tag{19}$$

where the inlet location, $x_i = -\infty$ (or $\overline{x_i} = -\frac{\pi}{2}$) for a fully flooded (drowned) inlet, and the exit position x_e ($\overline{x_e}$) is obtained by the solution of equation (18). Putting equation (19) in dimensionless form, using expressions in (12) and (13), substituting for p^* and noting that:

$$\overline{W} = \frac{Wh_0}{12lu\eta_0 R} \tag{20}$$

yields:

$$\overline{W} = \frac{1}{6} \left[\cos \bar{x} \right]_{-\frac{\pi}{2}}^{\frac{\pi}{e}} - \frac{w^*}{4\sqrt{2h_0^*}} \left[\bar{x} \right]_{-\frac{\pi}{2}}^{\frac{\pi}{e}}$$
 (21)

For pure rolling, $w^* = 0$ and with Swift [42]- Stieber [43] film rupture exit boundary condition (from equation (18):

$$\overline{x_e} = tan^{-1}(0.475129) \tag{22}$$

Thus, for steady-state condition (no squeeze film effect, and u = const), the contact reaction becomes:

$$W = \frac{2.8lu\eta_0 R}{h_0} \tag{23}$$

Squeeze film effect takes into account transient conditions affecting any variations in the gap (lubricant film thickness): $w = \frac{dh_0}{dt} = \dot{h_0}$. As already noted, $\overline{x_e}$ alters according to the extent of squeeze. Therefore, the generated lubricant reaction under combined rolling and squeeze film motion becomes:

$$W = \frac{2.8 lu \eta_0 R}{h_0} - \frac{3 l \eta_0 R^{3/2} h_0}{\sqrt{2} h_0^{3/2}} \left(\overline{x_e} + \frac{\pi}{2} \right)$$
 (24)

3.2- Iso-viscous lubricant: Stiffness and damping characteristics

Stiffness and damping characteristics of lubricated contacts can be obtained as:

$$k = \frac{\partial W}{\partial h_0}$$
 and $c = \frac{\partial W}{\partial \dot{h_0}}$ (25)

Under steady-state condition (pure rolling: pure lubricant entraining motion), using equation (23):

$$k = -\frac{2.8lu\eta_0 R}{h_0^2} \text{ and } c = 0$$
 (26)

This indicates that thinner films have a higher stiffness and an increased load carrying capacity.

The situation is more complex with squeeze film motion, which also contributes to the film stiffness as well as to conjunctional damping. Furthermore, it is not possible to separate these dynamic characteristics (stiffness and damping). Using equation (24):

$$k = \frac{9\sqrt{2}l\eta_0 R^{3/2}h_0(\overline{x_e} + \frac{\pi}{2})}{4h_0^{1/2}} - \frac{2.8lu\eta_0 R}{h_0^2}$$
(27)

$$c = \frac{3l\eta_0 R^{3/2}}{\sqrt{2}h_0^{3/2}} \left(\overline{x_e} + \frac{\pi}{2}\right) \tag{28}$$

Lubricant stiffness is enhanced by the squeeze film effect, $\dot{h_0} < 0$ (equation (27)), and reduced by separation of surfaces, denoted by $\dot{h_0} > 0$. With squeeze film motion, there is fluid film damping (equation (28)) as a function of $\overline{x_e}$ which increases with $\dot{h_0} < 0$. For pure squeeze, damping contribution attains its maximum value, where $\overline{x_e}$ can be replaced by $\frac{\pi}{2}$.

Figures 4(a) and 4(b) show the stiffness and damping characteristics for the conditions in Figure 3. It can be seen that the contact stiffness increases with a reducing film thickness. Furthermore, as w^* increases negatively (increased squeeze: normally approaching surfaces), the contact stiffness increases as the load carrying capacity is enhanced (figure 4(a)). Conversely, with increasingly positive values of w^* (contact separation), the contact stiffness is reduced. Interestingly, with thicker films the effect of squeeze film action diminishes as the stiffness becomes mainly due to pure rolling action. Similar characteristics are also noted for the case of contact viscous damping (figure 4(b)).

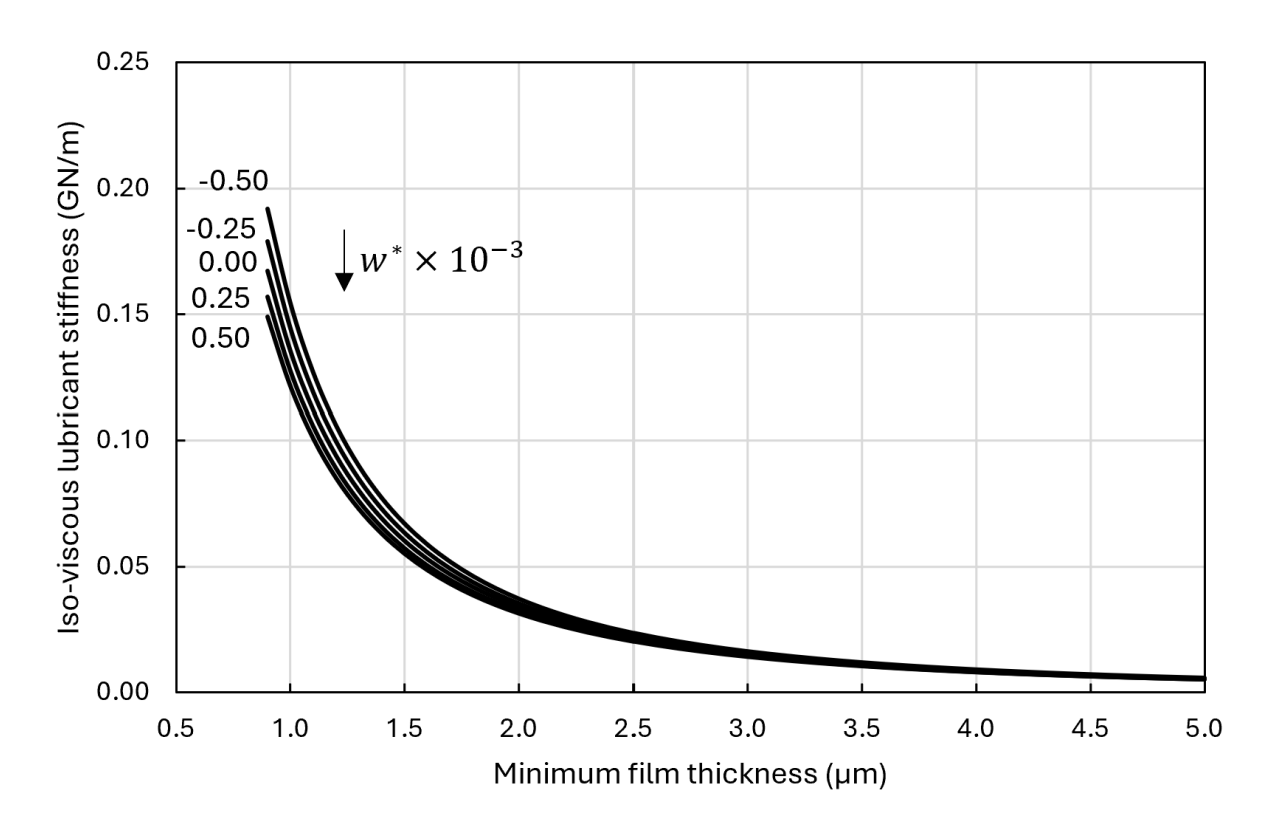


Figure 4(a): Variation of stiffness characteristics with increased film thickness and squeeze-roll speed ratio

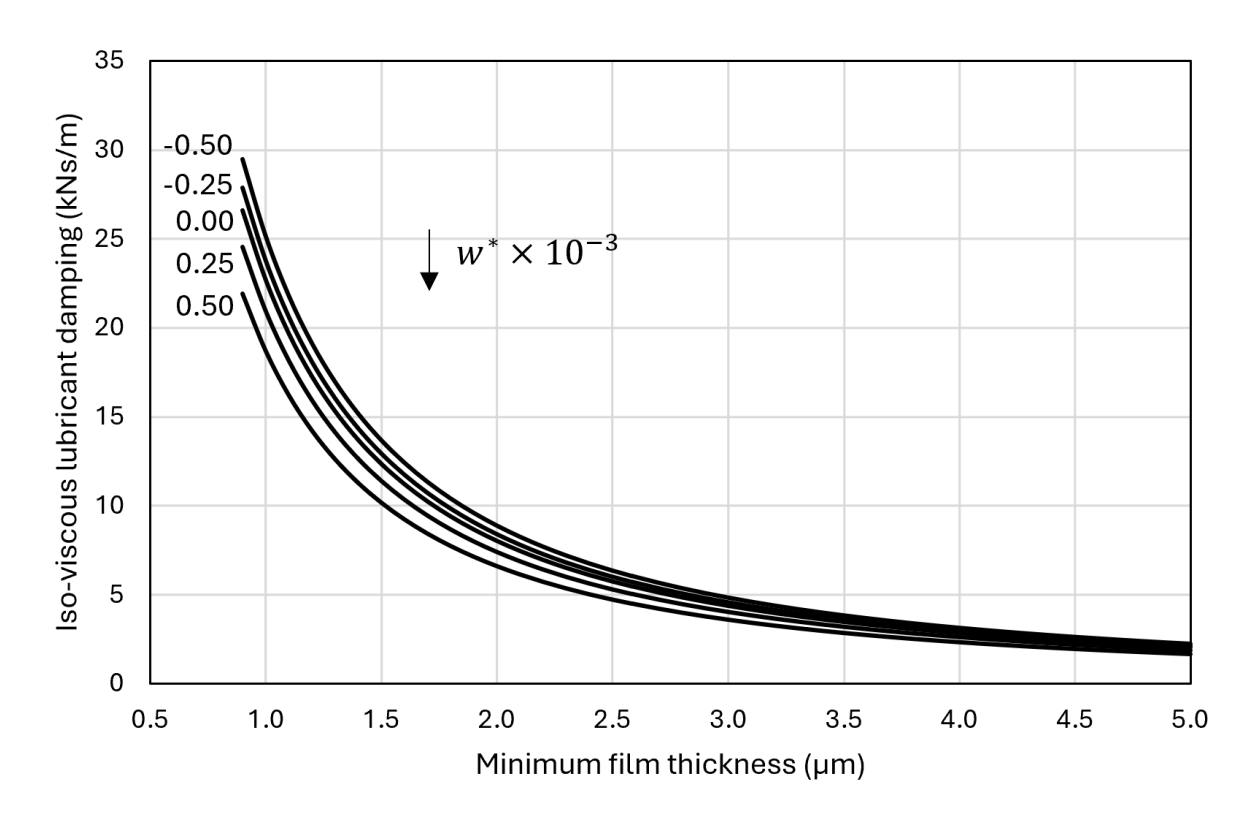


Figure 4(b): Variation of viscous damping with film thickness and squeeze-roll speed ratio

Iso-viscous rigid regime of lubrication occurs in light-to-medium loaded contacts where the generated pressures are insufficient to invoke the piezo-viscous action of the lubricant. A large range of lubrication problems arise where piezo-viscous rigid conditions occur.

3.3- Piezo-viscous condition: Pressure distribution and load carrying capacity

Lubricant viscosity increases with pressure. The rise in viscosity can be obtained using Barus law [44]:

$$\eta = \eta_0 e^{\alpha q} \tag{29}$$

where α is the piezo-viscosity of the lubricant. Replacing for η from equation (26) in the pressure gradient:

$$e^{-\alpha q} \frac{\partial q}{\partial x} = 6u \eta \frac{h - h_a}{h^3} = \frac{\partial p}{\partial x}$$
 (30)

A relationship between q and p can be obtained by integrating the left-hand side of equation (30), yielding the term: $-\frac{1}{\alpha}e^{-\alpha q} + C$. The constant of integration C is obtained such that as $q \to 0$, the entire term diminishes. Thus: $C = \frac{1}{\alpha}$. Now replacing the left-hand side term into equation (30) yields:

$$q = -\frac{1}{\alpha} \ln(1 - \alpha p) \tag{31}$$

Clearly, iso-viscous pressures that satisfy the mathematical restrictions: $\alpha p < 1$ yield feasible results, from which piezo-viscous pressures, q, can be obtained using equation (31). This restriction effectively introduces a limiting lubricant film thickness below which pressures, q, are deemed as excessive (exceeding hydrodynamic lubrication). Figure 4 shows the results for various squeeze-roll speed ratios, w^* , with a minimum dimensionless film thickness of $h_0^* = 70 \times 10^{-6}$ and dimensionless speed parameter, $u^* = \frac{u \eta_0 \alpha}{R} = 0.9 \times 10^{-6}$. They correspond to the iso-viscous results shown in figure 3.

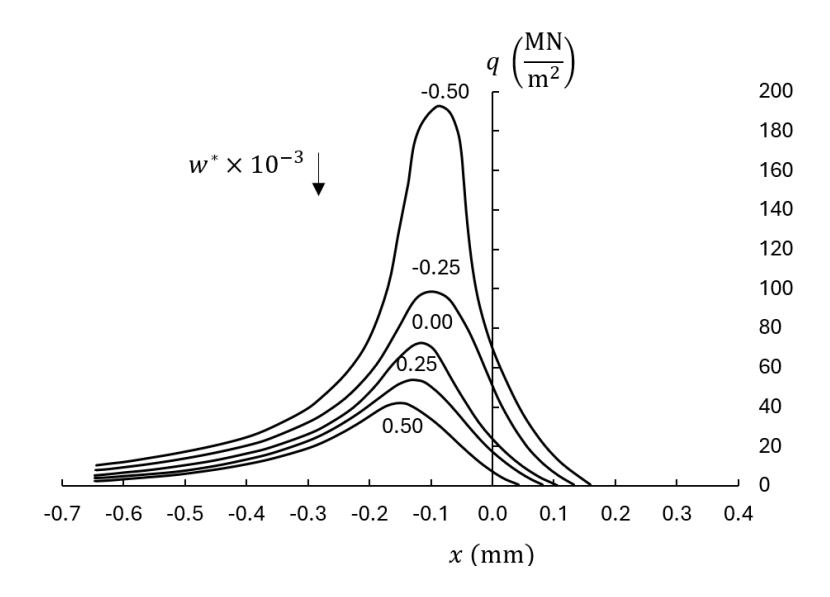


Figure 5: Actual piezo-viscous pressure distribution (combined Reynolds condition and squeeze film effect)

Similar results are obtained for various combinations of h_0^* , u^* and w^* through the determination of q and contact load from equation (19) (where p is replaced by q). Using regression analysis of all the numerical results, a relationship for minimum lubricant film thickness is obtained as:

$$h_0^* = 0.787u^{*0.7}\overline{W}^{-0.4}e^{-281.2w^*}$$
(32)

To date, this is the only piezo-viscous hydrodynamic rigid line contact film thickness equation for transient combined entraining and squeeze film motions.

A number of noteworthy observations can be made. The inverse proportionality of film thickness with contact load ($h_0 \propto W^{-1}$, see equation (23)) under iso-viscous condition is replaced by $h_0 \propto W^{-0.4}$. This indicates an increased contact stiffness, k (equation (22)). The lubricant film has begun to become less sensitive to the applied load. In fact, the exponent of \overline{W} reduces further with conditions pertaining to piezo-viscous elastic (i.e. elastohydrodynamics: EHD) as shown by the very first equation obtained by Grubin [45]:

$$h_0^* = 2.076u^{*0.72} \overline{W}^{-0.091} \tag{33}$$

The lubricant stiffness increases so dramatically that it becomes almost insensitive to load ($h_0 \propto \overline{W}^{-0.091}$). The lubricant is said to have become an amorphous solid.

4- Light-to-medium loaded rattle of loose gear pairs

Returning to the equation of motion (1) for a pair of impacting loose gear teeth, it is clear that the lubricant reaction, W(t), depends on the magnitude of applied load, F(t). When this impact load is insufficient to promote piezo-viscous action of the lubricant, transient iso-viscous hydrodynamics occur. Such conditions take place at low loads with low engine torque, representative of vehicle idling condition. The impact force is oscillatory, owing to the resident vibration on the transmission input shaft because of engine order vibrations [46]:

$$F(t) = Q + F_0 \cos 2\pi f_{exc} t \tag{34}$$

where Q is the steady state applied load with a superimposed oscillatory force at the excitation frequency of f_{exc} . The excitation frequency comprises vibrations resident on the engine crankshaft (transmitted to the transmission input shaft, see figure 1). These comprise imbalanced inertial dynamics spectrum of the piston-connecting rod- crankshaft system vibration superimposed on the signature of the combustion process itself [46]. For simplicity, only the fundamental excitation frequency of the spectral response is taken into account in the current analysis. The oscillatory nature of the impact force of loose gears is the major underlying cause of transmission rattle. The problem of oscillatory transmitted impact force is not only confined to the ICE powertrain systems. Hybrid powertrains and fully electric axles also suffer from this phenomenon [47-50].

As a pair of gears are engaged and subjected to medium contact loads, the nature of gear rattle alters with somewhat reduced vibration because of the piezo-viscous action of the lubricant. This form of rattle is termed creep rattle. Owing to higher engine noise at the onset of vehicle launch, creep rattle is less discernible than the idle rattle. In fact, some degree of rattle exists in all drive conditions, even under heavily loaded gear pairs where the condition is termed drive rattle [7, 8]. Therefore, rattle exists under various regimes of lubrication, from iso-viscous rigid through to elastohydrodynamics, as investigated and shown by De la Cruz et al [7]. It is clear that the lubricant plays a significant role in all the variants of rattle phenomenon. In the automotive industry an issue of interest has always been the determination of an acceptable threshold for transmission idle and creep rattles (i.e. at low to medium oscillating contact loads). A fundamental study of lubricant behaviour under such conditions is long overdue and is, therefore, one of the main contributions of the current study.

4.1- Idle gear rattle under iso-viscous contact condition

Referring back to the equation of motion (1), the oscillatory contact force: $F = Q + F_0 cos 2\pi f_{exc} t$ is used together with equation (24) for transmission system in idle condition. The equation of motion becomes:

$$\ddot{z}(i,j) = \frac{1}{m} \left\{ \frac{2.8 l u \eta_0 R}{h_0 + z(i,j)} - \frac{3\pi l \eta_0 R^{3/2} \dot{z}(i,j)}{\sqrt{2} (h_0 + z(i,j))^{3/2}} - Q - F_0 \cos 2\pi f_{exc} t \right\} - g$$
(35)

The movement of the roller centre, z, is transmitted directly to the surface of the lubricant film as under hydrodynamic conditions the roller surface remains rigid (see section 2). Therefore, a solution to system dynamics may be obtained in terms of the ripple oscillations of the lubricant film surface, z(t).

The counter i denotes the time step of simulation and j is the iteration counter within each step of integration time. The following convergence criterion should be met:

$$|z(i,j) - z(i,j-1)| < \varepsilon \tag{36}$$

where ε is the error tolerance, usually in the range $10^{-8} - 10^{-7}$ m.

The solution is obtained by adopting Newmark's average acceleration method [51], as highlighted in [52]. At the outset of simulation, pure rolling condition is assumed at a steady film thickness of h_0 ($z_0 = \dot{z_0} = 0, t = 0$).

Typical conditions pertaining to idle rattle condition are used in the case study. Figure 6 shows the oscillatory applied force with a forcing frequency of $f_{exc} = 600 \, Hz$ (FFT of the applied force is shown in figure 7). The equivalent mass of a gear impacting its conjugate pair is $m = 3 \, kg$ with the lubricant dynamic viscosity of $\eta_0 = 0.3 \, Pas$. The variation in the lubricant film thickness, $h_0 + z(i,j)$, is also shown in figure 6.

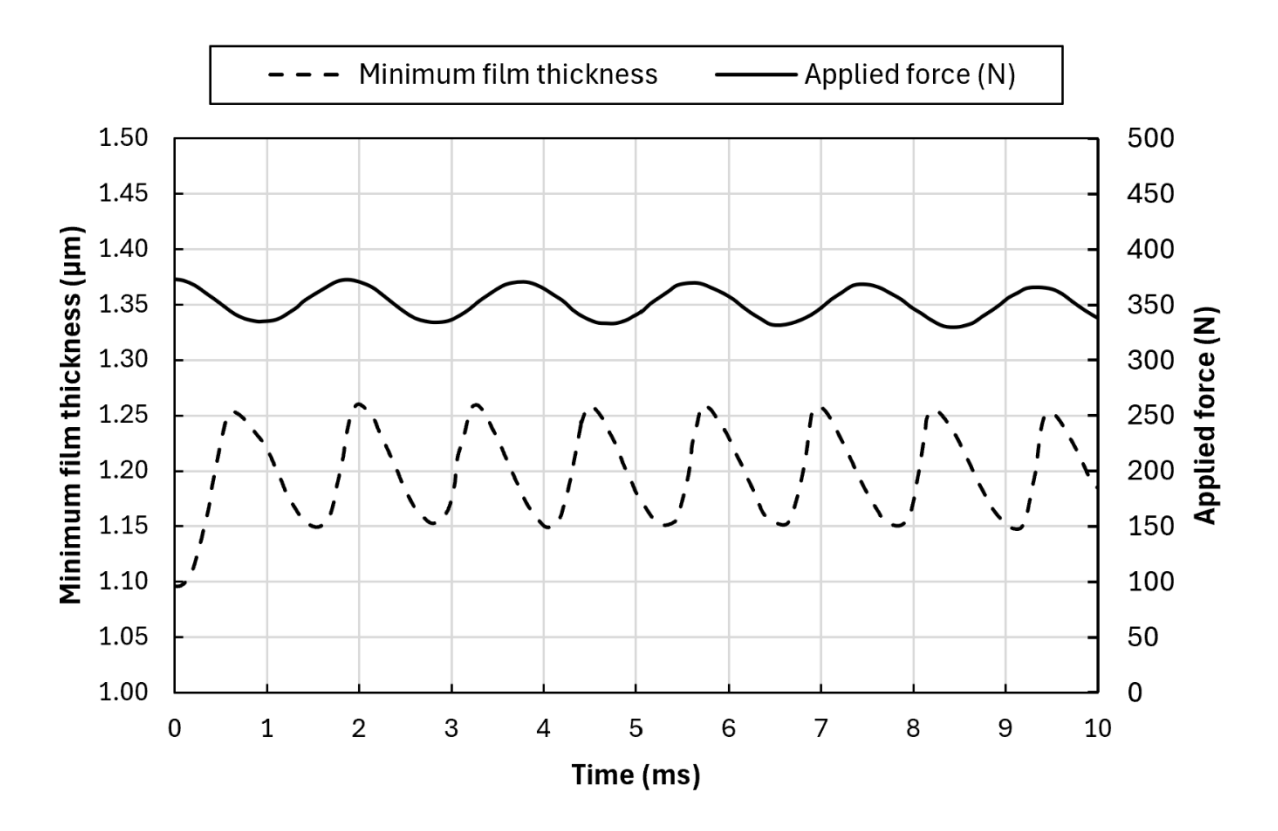


Figure 6: Film thickness variation under oscillatory applied forcing

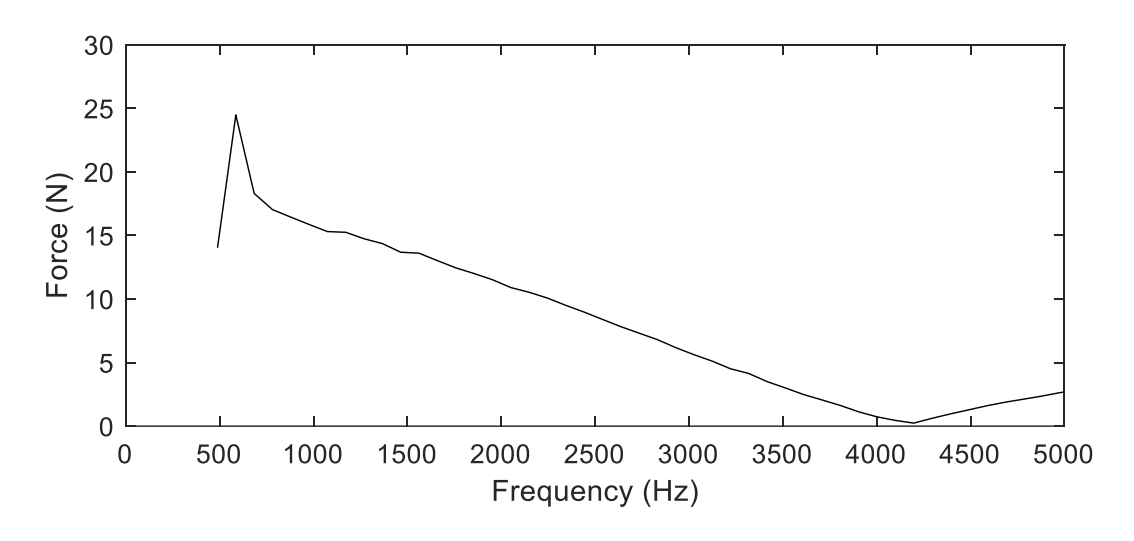


Figure 7: Spectrum of vibration of input forcing function

A clearer picture emerges when the time history of lubricant surface ripple acceleration, $\ddot{z}(i,j)$, is studied (see figure 8). This shows an oscillatory response with each cycle of oscillations, preceded by many low amplitude lubricant surface reversals. These provide strong evidence of rattling gear pairs under idle rattle, noted by various authors [1-6, 8]. They occur as the result of poor lubricant film load carrying capacity under iso-viscous conditions and are a sign of dynamic instability.

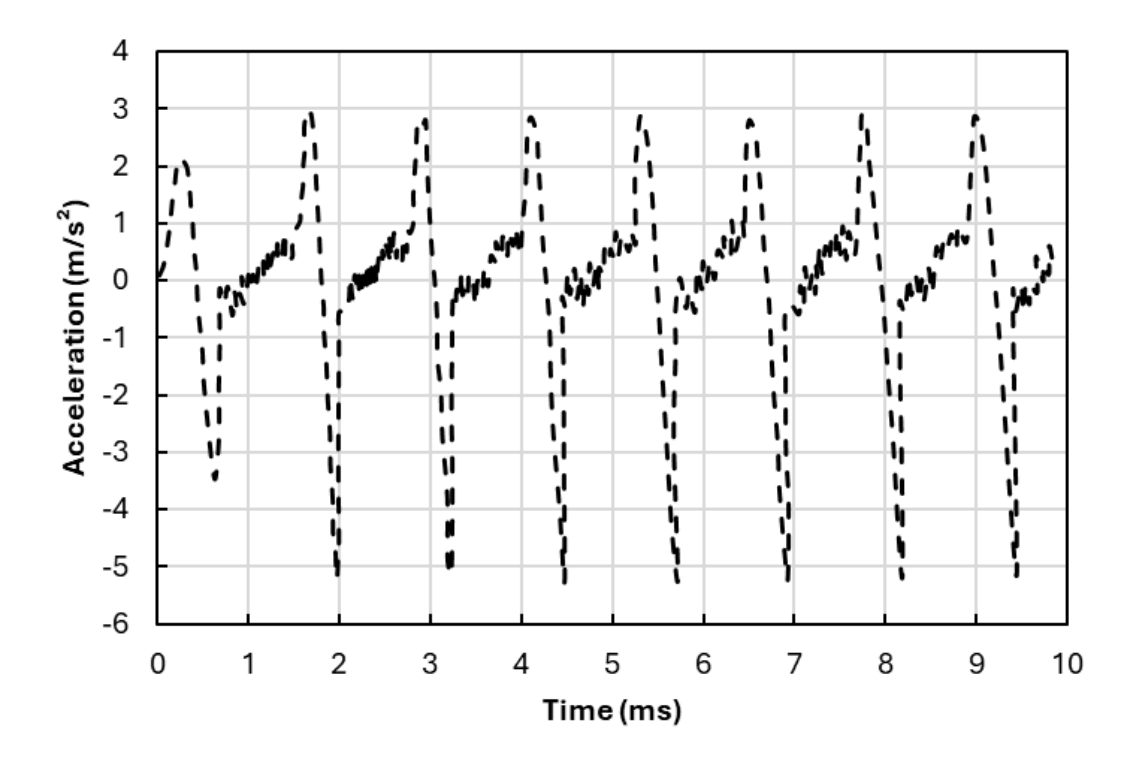


Figure 8: Time history of lubricant surface ripple acceleration under iso-viscous idle rattle

4.2- Creep rattle of a gear pair under piezo-viscous contact condition

Transmission creep rattle occurs at vehicle take-off (launch) in an engaged (selected) gear pair [8]. The rattle condition is initially at medium load with piezo-viscous lubricant behaviour, where the lubricant reaction is obtained by inverting equation (32), thus:

$$\ddot{z}(i,j) = \frac{1}{m} \left\{ \frac{6.6(u\eta_0)^{11/4}(R\alpha)^{7/4}}{(h_0 + z(i,j))^{7/2}e^{\left(\frac{703\dot{z}(i,j)}{u}\right)}} - Q - F_0 \cos 2\pi f_{exc} t \right\} - g$$
(37)

Step-by-step iterative solution of the equation of motion is obtained using Newmark's average acceleration method.

Figure 9 shows the time history of lubricant film surface ripple acceleration under the same loading condition as that under iso-viscous behaviour (figure 8). There is an absence of repetitive reversals owing to the increased load carrying capacity (lubricant reaction) that results from the piezo-viscous action of the lubricant.

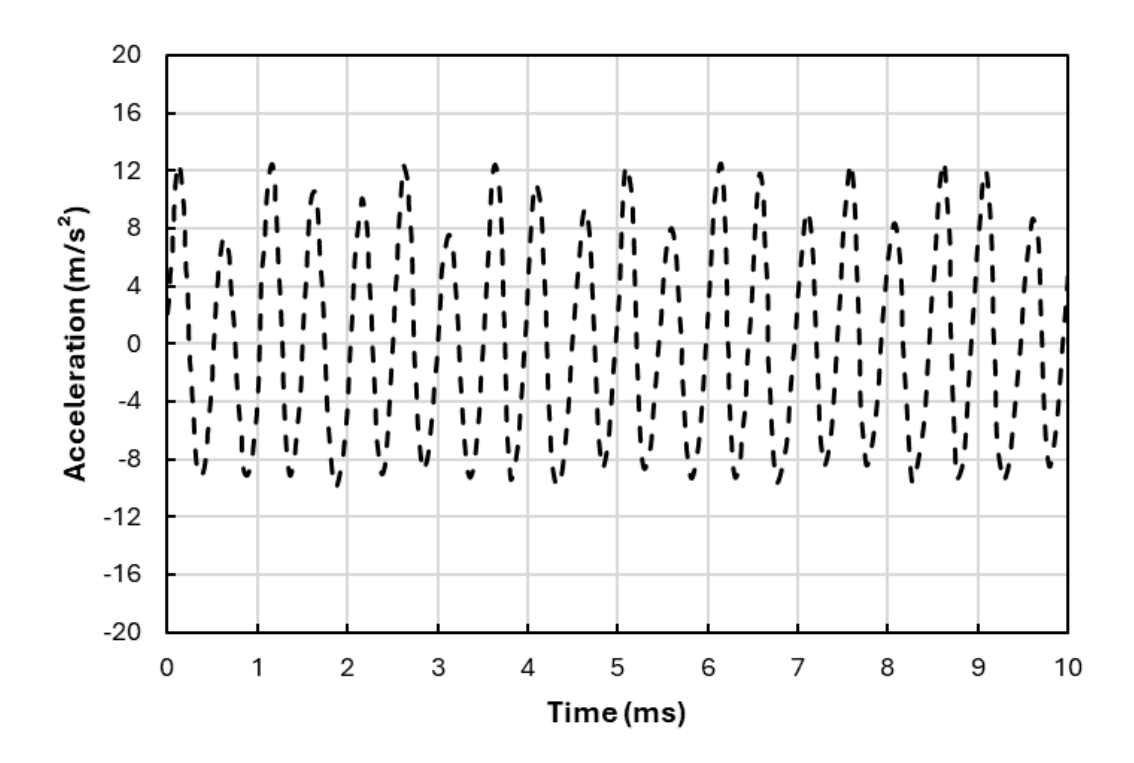


Figure 9: Time history of lubricant surface ripple acceleration under piezo-viscous creep rattle

Figures 10(a) and 10(b) show the spectrum of vibration of lubricant surface oscillations under isoviscous (figure 8) and piezo-viscous (figure 9) responses. The horizontal axis provides the ratio $\frac{f}{f_{exc}}$. Figure 10(a) shows that iso-viscous lubricant behaviour occurs at the forcing frequency and at a host of its higher harmonics. The existence of these higher harmonics is a clear sign of instability and low load carrying capacity. In contrast, figure 10(b) shows much reduced spectral content, with a response at the forcing frequency and a main contribution at $f \approx 2.5 f_{exc}$ which is the lightly damped natural frequency of the piezo-viscous lubricated contact. There are also smaller spectral contributions as the result of modulations between f and f_{exc} . This is a much more stable response than that in figure 10(a).

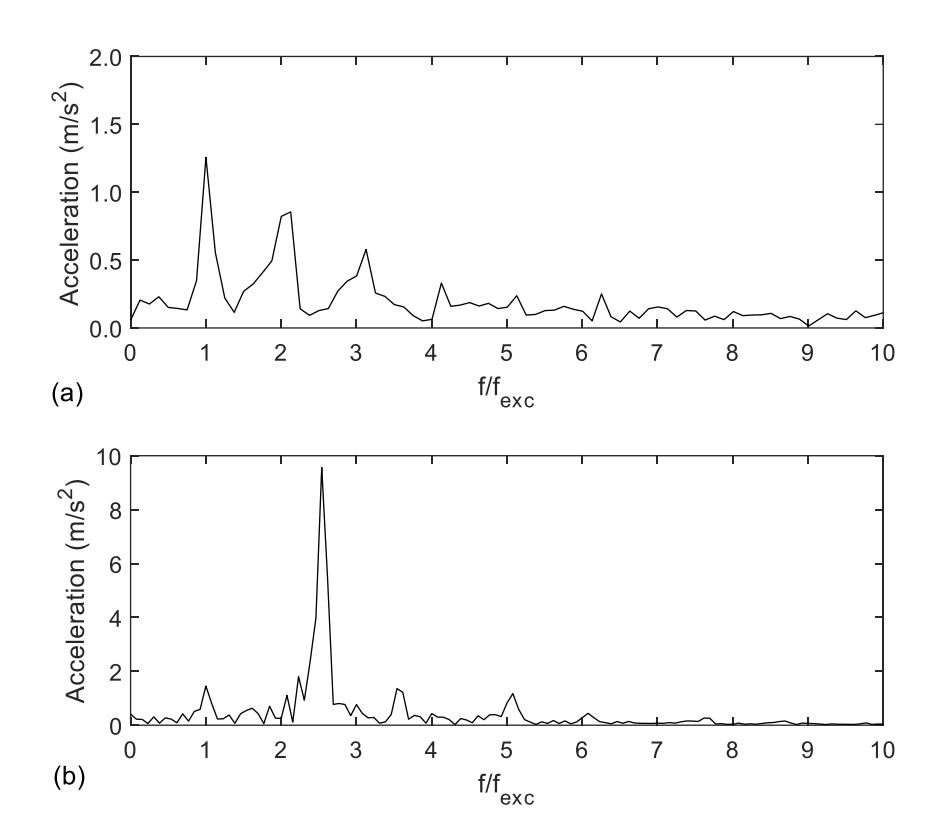


Figure 10: Spectrum of vibration of rattle response; (a) with iso-viscous lubricant behaviour; (b) with piezo-viscous lubricant action

5- Conclusions

The paper investigates the role of lubricant in the transient impact of loose gear teeth pairs under light to medium oscillatory loads, pertaining to gear rattle. Analytical solutions of Reynolds equation for non-conforming line contact of cylindrical pairs subjected to combined rolling and squeeze film motions are obtained. Cases of iso-viscous, as well as piezo-viscous, hydrodynamic lubricant behaviour are considered. These conditions correspond to low to medium loaded rigid body contacts. Lubricant reaction under these conditions is obtained through direct analytical derivation in the case of iso-viscous hydrodynamics [28] and through regression of results for piezo-viscous lubricant action. In the latter case, the lubricant film thickness equation is the first extrapolated equation reported for piezo-viscous hydrodynamic behaviour under transient counterformal line contacts (including the effect of squeeze film action and contact separation).

The non-linear integrated nature of lubricant stiffness and damping characteristics is demonstrated. These characteristics show enhanced potency with squeeze film action, indicating improved contact

load carrying capacity with squeeze film effect. This finding has been noted by other researchers but has not hitherto been clearly demonstrated in a fundamental manner as presented here.

The case of gear rattle is the most pertinent application of low to medium transient hydrodynamic action. Rattle has been and remains a main source of concern for all gearing systems, not least in the automotive industry as it is often seen as an indication of poor build quality. Using the developed methodology, cases of transmission rattle under low load (idle gear rattle), and under medium load at the onset of vehicle launch (creep rattle), are fundamentally investigated by tribodynamic solution of gear teeth pair interactions. It is shown that isothermal iso-viscous hydrodynamic lubricant behaviour is the underlying cause of idle gear rattle, where unstable transient lubricant behaviour occurs due to its poor load carrying capacity with many lubricant surface oscillatory reversals. More stable piezo-viscous lubricant behaviour is the underlying cause of creep rattle response. Although significant attention has been paid to the rattle response of gearing systems previously, the underlying behaviour of the lubricant has remained fundamentally unexplained prior to the current analyses.

Acknowledgements

The authors wish to express their gratitude to the Engineering and Physical Sciences Research Council, Ford Motor Company and Mechanical Dynamics Ltd for the funding of "Automotive Transmission Rattle" (EP/D050332/1), which has underpinned the current research methodology. Thanks are also extended to the British Ministry of Defence (Royal Aircraft Establishment: RAE) for the initial funding and technical support of the project on "Influence of vibration on lubricant film behaviour".

Nomenclature

Roman Symbols:

c Damping constant

E Young's modulus of elasticity

f Response frequency

 f_{exc} Frequency of excitation

 F_0 Magnitude of applied oscillatory impact force

g Gravitational acceleration

h Film thickness

24. Accepted version

h_0	Minimum film thickness
h_a	Film thickness at maximum pressure
k	Lubricant contact stiffness
l	Contact length
m	Equivalent mass
p	Iso-viscous Pressure (reduced pressure)
p_0	Maximum pressure
q	Piezo-viscous pressure
Q	Steady state applied force
R	Radius of an equivalent ellipsoidal solid near a semi-infinite half-space
$r_{1.2}$	Radii of right circular cylinders at their contact
t	Time
u	Speed of entraining motion
$u_{1,2}$	Surface speed of contacting surfaces
W	Contact load
W	Squeeze velocity
$W_{1,2}$	Velocity of normal approach of contacting surfaces
x	Direction of entraining motion
$-x_a$	Position of maximum pressure
x_e	Position of lubricant film rupture
z	Displacement in the direction of normal approach and separation
Ż	Squeeze film/ normal lubricant surface speed
\ddot{z}	Acceleration of normal approach and separation

Greek Symbols:

α Pressure-viscosity coefficient

 δ Elastic deflection

Error tolerance in convergence criterion

 η Dynamic viscosity

 η_0 Atmospheric dynamic viscosity

θ Poisson's ratio

Non-dimensional variables

*p** Dimensionless pressure

*u** Dimensionless speed parameter

 \overline{W} Dimensionless load parameter

*w** Squeeze-roll speed ratio

 \bar{x} Dimensionless distance

References

- [1]- Theodossiades, S., Tangasawi, O. and Rahnejat, H., "Multi-physics approach for analysis of transmission rattle", In Tribology and Dynamics of Engine and Powertrain, Woodhead Publishing, 2010, pp. 878-913.
- [2]- Brancati, R., Rocca, E. and Russo, R., "A Gear Rattle Model Accounting for Oil Squeeze Between the Meshing Gear Teeth", Proc. IMechE Part D: J. Automobile Engineering, 2005, 219, pp. 1075-1083.
- [3]- Tangasawi, O., Theodossiades, S. and Rahnejat, H., "Lightly loaded lubricated impacts: idle gear rattle", J. Sound and Vibration, 2007; 308(3-5), pp. 418-430.
- [4]- Doğan, S.N., "Rattle and clatter noise in powertrains—automotive transmissions", In Tribology and Dynamics of Engine and Powertrain, Woodhead Publishing, 2010, pp. 793-838.
- [5]- Baumann, A. and Bertsche, B., "Experimental study on transmission rattle noise behaviour with particular regard to lubricating oil", J. Sound and Vibration, 2015, 341, pp. 195-205.
- [6]- Rahnejat, H., Theodossiades, S., Kelly, P. and Menday, M.T., "Drivetrain noise, vibration, and harshness", Encyclopedia of Automotive Engineering, 2014, 17:1
- [7]- De la Cruz, M., Theodossiades, S. and Rahnejat, H., "An investigation of manual transmission drive rattle", Proc. IMechE, Part K: J. Multi-body Dynamics, 2010, 224(2), pp. 167-181.

- [8]- Menday, M., "An introduction to noise and vibration issues in the automotive drivetrain and the role of tribology", Tribology and Dynamics of Engine and Powertrain, Woodhead Publishing, 2010, pp. 663-679.
- [9]- Teodorescu, M., Taraza, D., "Combined multi-body dynamics and experimental investigation for determination of the cam-flat tappet contact condition", Proc. IMechE, Part K: J Multi-body Dynamics. 2004, 218(3), pp. 133-142.
- [10[- Kushwahu, M., "Tribological issues in cam-tappet contacts", In Tribology and Dynamics of Engine and Powertrain, Woodhead Publishing, 2010, pp. 545-566.
- [11]- Chong, W.W.F., Teodorescu, M. and Rahnejat, H., "Mixed thermo-elastohydrodynamic camtappet power loss in low-speed emission cycles", Int. J. Engine Research, 2014, 15(2), pp. 153-164.
- [12]- Shirzadegan, M., Almqvist, A. and Larsson, R., "Fully coupled EHL model for simulation of finite length line cam-roller follower contacts", Tribology Int., 2016, 103, pp. 584-598.
- [13]- Li, S. and Kahraman, A., "A tribo-dynamic model of a spur gear pair", J. Sound and Vibration, 2013, 332(20), pp. 4963-4978.
- [14]- Li, S. and Kahraman, A., "Prediction of spur gear mechanical power losses using a transient elastohydrodynamic lubrication model", Tribology Transactions, 2010, 53(4), pp. 554-563.
- [15]- Sivayogan, G., Rahmani, R. and Rahnejat, H., "Lubricated loaded tooth contact analysis and non-Newtonian thermoelastohydrodynamics of high-performance spur gear transmission systems", Lubricants, 2020, 8(2): 20.
- [16]- Ankouni, M, Lubrecht, A.A. and Velex, P., "Modelling of damping in lubricated line contacts—Applications to spur gear dynamic simulations", Proc. IMechE, Part C: J. Mechanical Engineering Science, 2016, 230(7-8), pp. 1222-1232.
- [17]- Sivayogan, G., Dolatabadi, N., Johns-Rahnejat, P., Rahmani, R. and Rahnejat, H., "Non-Newtonian thermo-elastohydrodynamics and sub-surface stress field of high-performance racing spur gears", Lubricants, 2022, 10(7):146.
- [18]- Liao, K., Liu, Y., Kim, D., Urzua, P. and Tian, T., "Practical challenges in determining piston ring friction", Proc. IMechE, Part J. J. Engineering Tribology, 2013, 227(2), pp. 112-125.
- [19]- D'Agostino, V. and Senatore, A., ""Fundamentals of lubrication and friction of piston ring contact", Tribology and Dynamics of Engine and Powertrain—fundamentals, applications and future trends, Woodhead Publishing, 2010, pp. 343-383.
- [20]- Baker, C., Theodossiades, S., Rahmani, R., Rahnejat, H. and Fitzsimons, B., "On the transient three-dimensional tribodynamics of internal combustion engine top compression ring", J. Engineering for Gas Turbines and Power, 2017, 139(6): 062801.
- [21]- Meng, Z., Tian, T. and Lubrecht, T., "A numerical model for piston pin lubrication in internal combustion engines", SAE Technical Paper, No. 2020-01-2228, 2020.
- [22]- Shu, Z., Tian, T., Meng, Z., Fiedler, R.G. and Berbig, F,."Modeling of piston pin rotation in a large bore gas engine", SAE Technical Paper, No. 2023-32-0161, 2023
- [23]- Stacke, L.E., Fritzson, D. and Nordling, P., "BEAST—a rolling bearing simulation tool", Proc. IMechE, Part K: J. Multi-body Dynamics, 1999, 213(2), pp. 63-71.

- [24]- Gupta, P.K., "Dynamics of rolling-element bearings—part II: cylindrical roller bearing results", J. Lubrication Tech., 1979, 101(3), pp. 305-311.
- [25]- Kushwaha, M. and Rahnejat, H., "Transient concentrated finite line roller-to-race contact under combined entraining, tilting and squeeze film motions", J. Physics D: Applied Physics, 2004, 37(14): 2018.
- [26]- Mohammadpour, M., Johns-Rahnejat, P.M. and Rahnejat, H., "Roller bearing dynamics under transient thermal-mixed non-Newtonian elastohydrodynamic regime of lubrication", Proc. IMechE, Part K: J. Multi-body Dynamics, 2015, 229(4), pp. 407-423.
- [27]- Herrebrugh, K., "Elastohydrodynamic squeeze films between two cylinders in normal approach", J. Lubrication Tech., 1970, 92(2), pp. 292-301
- [28]- Rahnejat, H., "Influence of vibrations on the oil film in concentrated contacts", PhD thesis, Imperial College, University of London, 1984.
- [29]- Taylor, R.I., "Squeeze film lubrication in piston rings and reciprocating contacts", Proc. IMechE, Part J: J. Engineering Tribology, 2015, 229(8), pp. 977-988.
- [30]- Gohar, R. and Rahnejat, H., "Fundamentals of Tribology", 3rd edition, World Scientific, London, 2018.
- [31]- Rahnejat, H. and Gohar, R., "The vibrations of radial ball bearings", Proc. IMechE, Part C: J. Mechanical Engineering Science, 1985, 199(3), pp. 181-193.
- [32]- Qin, W., Chao, J. and Duan, L., "Study on stiffness of elastohydrodynamic line contact", Mechanism and Machine Theory, 2015, 86, pp. 36-47.
- [33]- Zhang, Y., Liu, H., Zhu, C., Liu, M. and Song, C., "Oil film stiffness and damping in an elastohydrodynamic lubrication line contact-vibration", J. Mechanical Science and Technology, 2016, 30, pp. 3031-3039.
- [34]- Zhou, C. and Xiao, Z., "Stiffness and damping models for the oil film in line contact elastohydrodynamic lubrication and applications in the gear drive", Applied Mathematical Modelling, 2018, 61, pp. 634-649.
- [35]- Tsuha, N.A. and Cavalca, K.L., "Finite line contact stiffness under elastohydrodynamic lubrication considering linear and nonlinear force models", Tribology Int., 2020,146: 106219.
- [36]- Fang, C., Zhu, A., Zhou, W., Peng, Y. and Meng, X., "On the stiffness and damping characteristics of line contacts under transient elastohydrodynamic lubrication", Lubricants, 2022, 10(4): 73.
- [37]- Dareing, D.W. and Johnson, K.L., "Fluid film damping of rolling contact vibrations", J. Mechanical Engineering Science, 1975, 17(4), pp. 214-218.
- [38]- Mehdigoli, H., Rahnejat, H. and Gohar, R., "Vibration response of wavy surfaced disc in elastohydrodynamic rolling contact", Wear, 1990, 139(1), pp. 1-5.
- [39]- Hamrock, B.J., "Fundamentals of Fluid Film Lubrication", Taylor and Francis, Roca Raton, 1991.
- [40]- Hertz, H., "Über die Berührung fester elastischer Körper", J reine und angewandte Mathematik, 1881, 92: 156.
- [41]- Dowson, D.. "A generalized Reynolds equation for fluid-film lubrication", Int. J. Mech. Sci., 1962, 4, pp. 159–170.

- [42]- Swift, H.W., "The stability of lubricating films in journal bearings", J. Institution of Civil Engineers, 1932, 233(1):267.
- [43]- Stieber, W., "Das Schwimmlager. Verein Deutscher", Berlin: Ingenieurre, 1933.
- [44]- Barus, C., "Fluid volume and its relation to pressure and temperature", American Journal of Science, 1890, 3(234), pp. 478-511.
- [45]- Grubin, A. N., "Contact Stresses in Toothed Gears and Worm Gears", Book 30 CSRI for Technology and Mechanical Engineering, Moscow, DSRI Trans,, 1949, No 337.
- [46]- Rahnejat, H., "Multi-body dynamics: vehicles, machines and mechanisms", Professional Engineering Publishing, Bury St Edmunds, UK, 1998.
- [47]- Zhang, J., Liu, D. and Yu, H., "Experimental and numerical analysis for the transmission gear rattle in a power-split hybrid electric vehicle", Int. J. Vehicle Design, 2017, 74(1), pp. 1-8.
- [48]- Hou L, Lei Y, Fu Y, Hu J. Effects of lightweight gear blank on noise, vibration and harshness for electric drive system in electric vehicles. Proc. IMechE, Part K: J. Multi-Body Dynamics, 2020, 234(3), pp. 447-464.
- [49]- Fabra-Rodriguez, M., Peral-Orts, R., Campello-Vicente, H. and Campillo-Davo, N., "Gear sound model for an approach of a Mechanical Acoustic Vehicle Alerting System (MAVAS) to increase EV's detectability", Applied Acoustics, 2021,184:108345.
- [50]- Wang, D., Zhang, W. and Yang, Z., "Analysis and Control of Gear Rattle Noise for E-Axle", SAE Technical Paper, No. 2023-01-7019, 2023.
- [51]- Newmark, N. M., "A method of computation for structural dynamics", J. Engineering Mechanics Division, ASCE, 1959, 85, pp. 67-94.
- [52]- Rahnejat, H., "Computational modelling of problems in contact dynamics", Engineering analysis, 1985, 2(4), pp. 192-197.